

# The Discontinuous Enrichment Method for Advection-Dominated Transport Phenomena in Computational Fluid Dynamics

**Irina Kalashnikova**<sup>1</sup>, R. Tezaur<sup>2</sup>, C. Farhat<sup>1,2</sup>

<sup>1</sup> Institute for Computational & Mathematical Engineering (iCME)

<sup>2</sup> Department of Aeronautics & Astronautics  
Stanford University

Bay Area Scientific Computing Day  
(BASCD 2011)  
Sunday, May 8, 2011



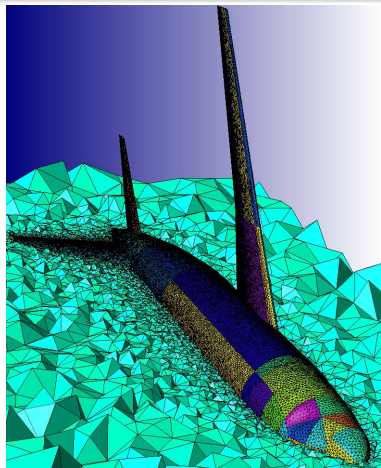
# Outline

- 1 Motivation
- 2 Advection-Diffusion Equation
- 3 Discontinuous Enrichment Method (DEM)
- 4 DEM for the 2D Constant-Coefficient Advection-Diffusion
  - Enrichment Basis
  - Lagrange Multiplier Approximations
  - Element Design
  - Numerical Results
- 5 DEM for 2D Variable-Coefficient Advection-Diffusion
  - Extension of Constant-Coefficient DEM Methodology
  - Numerical Results
- 6 DEM for 2D Unsteady Advection-Diffusion
  - Extension of Steady DEM Methodology
  - Numerical Results
- 7 Summary



# The Finite Element Method (FEM) in Fluid Mechanics

- Galerkin **Finite Element Method** (FEM) has a number of attractions in fluid mechanics:
  - Flexibility in handling complex geometries.
  - Ability to handle different forms of boundary conditions.
- FEM is quasi-optimal for elliptic (*diffusion*-dominated) PDEs: assures good performance of the computation at any mesh resolution.

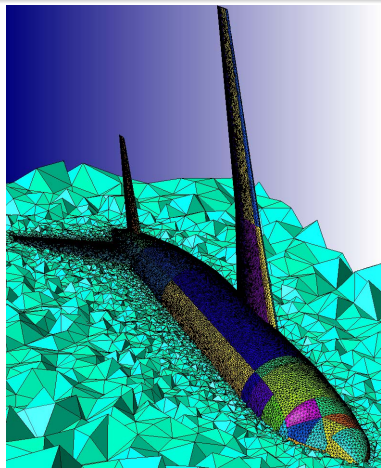


# The Finite Element Method (FEM) in Fluid Mechanics

- Galerkin **Finite Element Method** (FEM) has a number of attractions in fluid mechanics:
  - Flexibility in handling complex geometries.
  - Ability to handle different forms of boundary conditions.
- FEM is quasi-optimal for elliptic (*diffusion*-dominated) PDEs: assures good performance of the computation at any mesh resolution.

## However:

coarse mesh accuracy is not guaranteed when the flow is *advection*-dominated!





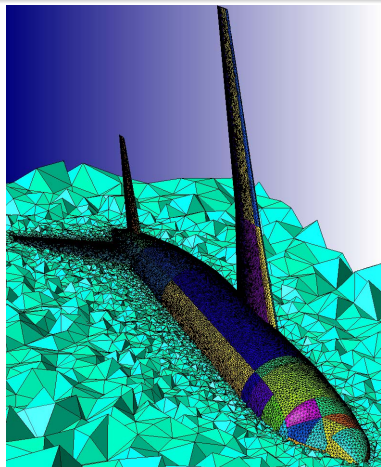
# The Finite Element Method (FEM) in Fluid Mechanics

- Galerkin **Finite Element Method** (FEM) has a number of attractions in fluid mechanics:
  - Flexibility in handling complex geometries.
  - Ability to handle different forms of boundary conditions.
- FEM is quasi-optimal for elliptic (*diffusion*-dominated) PDEs: assures good performance of the computation at any mesh resolution.

## However:

coarse mesh accuracy is not guaranteed when the flow is *advection*-dominated!

Significant mesh refinement typically needed to capture boundary layer region



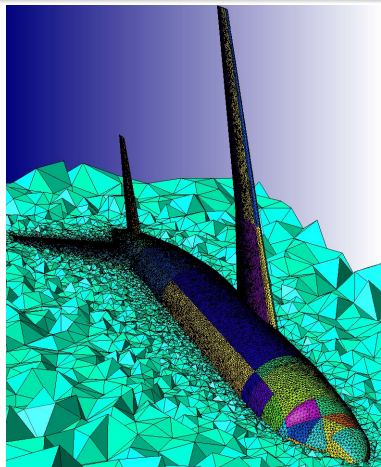
# The Finite Element Method (FEM) in Fluid Mechanics

- Galerkin **Finite Element Method** (FEM) has a number of attractions in fluid mechanics:
  - Flexibility in handling complex geometries.
  - Ability to handle different forms of boundary conditions.
- FEM is quasi-optimal for elliptic (*diffusion*-dominated) PDEs: assures good performance of the computation at any mesh resolution.

## However:

coarse mesh accuracy is not guaranteed when the flow is *advection*-dominated!

Significant mesh refinement typically needed to capture boundary layer region



**EXPENSIVE!**



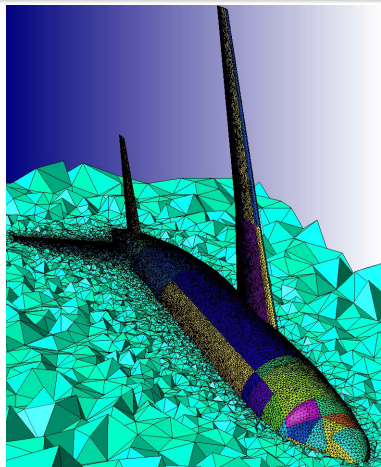
# The Finite Element Method (FEM) in Fluid Mechanics

- Galerkin **Finite Element Method** (FEM) has a number of attractions in fluid mechanics:
  - Flexibility in handling complex geometries.
  - Ability to handle different forms of boundary conditions.
- FEM is quasi-optimal for elliptic (*diffusion-dominated*) PDEs: assures good performance of the computation at any mesh resolution.

## However:

coarse mesh accuracy is not guaranteed when the flow is *advection-dominated*!

Significant mesh refinement typically needed to capture boundary layer region



**EXPENSIVE!**

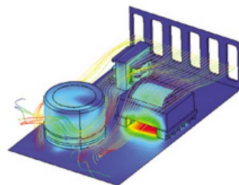
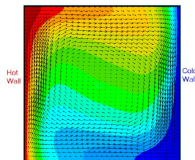
- **Approach:** develop a novel, efficient FEM that can accurately capture boundary layers for a canonical fluid problem; then generalize.



# Scalar Advection-Diffusion Equation

$$\mathcal{L}c = \underbrace{-\kappa \Delta c}_{\text{diffusion}} + \underbrace{\mathbf{a} \cdot \nabla c}_{\text{advection}} = f$$

- 2D advection velocity vector:  
 $\mathbf{a} = (a_1, a_2)^T = |\mathbf{a}|(\cos \phi, \sin \phi)^T$ .
- $\phi$  = advection direction.
- $\kappa$  = diffusivity.



- Describes many transport phenomena in fluid mechanics:
  - Heat transfer.
  - Semi-conductor device modeling.
  - Usual scalar model for the more challenging Navier-Stokes equations.
- Global **Péclet number** ( $L$  = length scale associated with  $\Omega$ ):

$$Pe = \frac{\text{rate of advection}}{\text{rate of diffusion}} = \frac{L|\mathbf{a}|}{\kappa} = Re \cdot \begin{cases} Pr & \text{(thermal diffusion)} \\ Sc & \text{(mass diffusion)} \end{cases}$$



# Advection-Dominated Regime

- Typical applications: flow is advection-dominated.

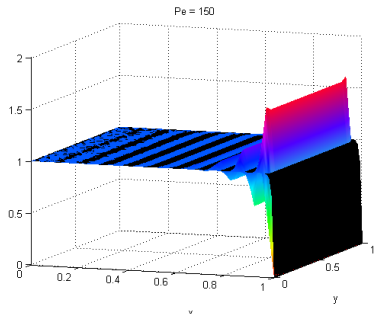


**Figure 1:** Galerkin  $Q_1$  solution (color) vs. exact solution (black) ( $Pe = 150$ )

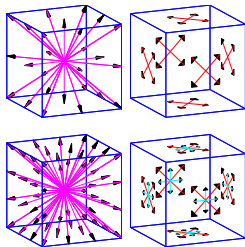
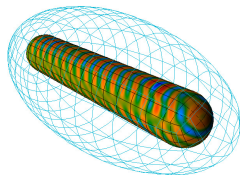
Advection-Dominated  
(High  $Pe$ ) Regime  
 $\Downarrow$   
 Sharp gradients in exact solution  
 $\Downarrow$   
 Galerkin FEM inadequate:  
 spurious oscillations (Fig. 1)

- Some classical remedies:
  - Stabilized FEMs** (SUPG, GLS, USFEM): add weighted residual (numerical diffusion) to variational equation.
  - RFB, VMS, PUM**: construct conforming spaces that incorporate knowledge of local behavior of solution.



# History of the Discontinuous Enrichment Method (DEM) and Its Success

- **Acoustic scattering problems** (Helmholtz equation) [4,5].
  - First developed by Farhat *et. al* in 2000 for the Helmholtz equation.
  - A family of 3D hexahedral DEM elements for medium frequency problems achieved the same solution accuracy as Galerkin elements of comparable convergence order using 4–8 times fewer dofs, and *up to 60 times less CPU time* [4].
  - Domain decomposition-based iterative solver for 2D and 3D acoustic scattering problems in medium- and high- frequency regimes has been developed [5].
- **Wave propagation in elastic media** (Navier's equation) [6].
- **Fluid-structure interaction problems** (Navier's equation and the Helmholtz equation) [7, 8].

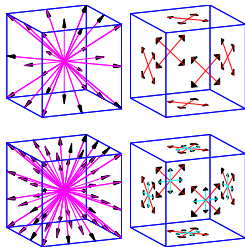
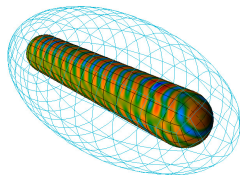


# History of the Discontinuous Enrichment Method (DEM) and Its Success

- **Acoustic scattering problems** (Helmholtz equation) [4,5].
  - First developed by Farhat *et. al* in 2000 for the Helmholtz equation.
  - A family of 3D hexahedral DEM elements for medium frequency problems achieved the same solution accuracy as Galerkin elements of comparable convergence order using 4–8 times fewer dofs, and *up to 60 times less CPU time* [4].
  - Domain decomposition-based iterative solver for 2D and 3D acoustic scattering problems in medium- and high- frequency regimes has been developed [5].
- **Wave propagation in elastic media** (Navier's equation) [6].
- **Fluid-structure interaction problems** (Navier's equation and the Helmholtz equation) [7, 8].

Excellent performance motivates development of DEM for other applications

→ **Fluid Mechanics**



# Enrichment Field in DEM

## Idea of DEM:

“Enrich” the usual Galerkin polynomial field  $\mathcal{V}^P$  by the free-space solutions to the governing homogeneous PDE  $\mathcal{L}c = 0$ .

$$c^h = c^P + c^E \in \mathcal{V}^P \oplus (\mathcal{V}^E \setminus \mathcal{V}^P)$$

where

$$\mathcal{V}^E = \text{span}\{c : \mathcal{L}c = 0\}$$

## • Simple 1D Example:

$$\begin{cases} u_x - u_{xx} = 1 + x, & x \in (0, 1) \\ u(0) = 0, u(1) = 1 \end{cases}$$

- *Enrichments:*  $u_x^E - u_{xx}^E = 0 \Rightarrow u^E = C_1 + C_2 e^x \Rightarrow \mathcal{V}^E = \text{span}\{1, e^x\}$ .
- *Galerkin FEM polynomials:*  $\mathcal{V}_{\Omega^e=(x_j, x_{j+1})}^P = \text{span}\left\{\frac{x_{j+1}-x}{h}, \frac{x-x_j}{h}\right\}$ .






# What about Inter-Element Continuity?

DEM = DGM with Lagrange Multipliers

- DEM is **discontinuous** by construction (enrichment field in DEM is *not* required to vanish at element boundaries).

---

<sup>1</sup>Necessary condition for generating a non-singular global discrete problem. 



# What about Inter-Element Continuity?

DEM = DGM with Lagrange Multipliers

- DEM is **discontinuous** by construction (enrichment field in DEM is *not* required to vanish at element boundaries).
- Continuity across element boundaries is enforced weakly using Lagrange multipliers  $\lambda^h \in \mathcal{W}^h$ :

$$\lambda^h \approx \nabla c_{\theta}^E \cdot \mathbf{n}^e = -\nabla c_{\theta'}^E \cdot \mathbf{n}^{e'} \quad \text{on } \Gamma^{e,e'}$$

*but making sure we uphold the...*

- Discrete **Babuška-Brezzi *inf-sup* condition**<sup>1</sup>:

$$\left\{ \begin{array}{l} \# \text{ Lagrange multiplier} \\ \text{constraint equations} \end{array} \leq \begin{array}{l} \# \text{ enrichment} \\ \text{equations} \end{array} \right\}$$

<sup>1</sup>Necessary condition for generating a non-singular global discrete problem.



# What about Inter-Element Continuity?

DEM = DGM with Lagrange Multipliers

- DEM is **discontinuous** by construction (enrichment field in DEM is *not* required to vanish at element boundaries).
- Continuity across element boundaries is enforced weakly using Lagrange multipliers  $\lambda^h \in \mathcal{W}^h$ :

$$\lambda^h \approx \nabla c_{\theta}^E \cdot \mathbf{n}^e = -\nabla c_{\theta'}^E \cdot \mathbf{n}^{e'} \quad \text{on } \Gamma^{e,e'}$$

*but making sure we uphold the...*

- Discrete **Babuška-Brezzi *inf-sup* condition**<sup>1</sup>:

$$\left\{ \begin{array}{l} \# \text{ Lagrange multiplier} \\ \text{constraint equations} \end{array} \leq \begin{array}{l} \# \text{ enrichment} \\ \text{equations} \end{array} \right\}$$

$$\Rightarrow n^\lambda = \left\lfloor \frac{n^E}{4} \right\rfloor$$

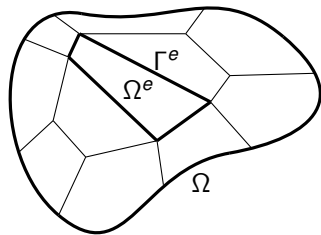
<sup>1</sup>Necessary condition for generating a non-singular global discrete problem.



# Hybrid Variational Formulation of DEM

- Strong form:

$$(S) : \left\{ \begin{array}{ll} \text{Find } \mathbf{c} \in H^1(\Omega) \text{ such that} \\ -\kappa \Delta \mathbf{c} + \mathbf{a} \cdot \nabla \mathbf{c} = f, & \text{in } \Omega \\ \mathbf{c} = g, & \text{on } \Gamma = \partial\Omega \end{array} \right.$$



## Notation:

$$\tilde{\Omega} = \bigcup_{e=1}^{n_{el}} \Omega^e$$

$$\tilde{\Gamma} = \bigcup_{e=1}^{n_{el}} \Gamma^e$$

$$\Gamma^{e,e'} = \Gamma^e \cap \Gamma^{e'}$$

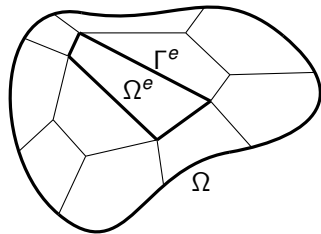
$$\Gamma^{\text{int}} = \bigcup_{e' < e} \bigcup_{e=1}^{n_{el}} \{\Gamma^e \cap \Gamma^{e'}\}$$



# Hybrid Variational Formulation of DEM

- Strong form:

$$(S) : \left\{ \begin{array}{ll} \text{Find } \mathbf{c} \in H^1(\Omega) \text{ such that} \\ -\kappa \Delta \mathbf{c} + \mathbf{a} \cdot \nabla \mathbf{c} = f, & \text{in } \Omega \\ \mathbf{c} = g, & \text{on } \Gamma = \partial\Omega \\ \mathbf{c}_e - \mathbf{c}_{e'} = 0, & \text{on } \Gamma^{\text{int}} \end{array} \right.$$



## Notation:

$$\tilde{\Omega} = \bigcup_{e=1}^{n_{el}} \Omega^e$$

$$\tilde{\Gamma} = \bigcup_{e=1}^{n_{el}} \Gamma^e$$

$$\Gamma^{e,e'} = \Gamma^e \cap \Gamma^{e'}$$

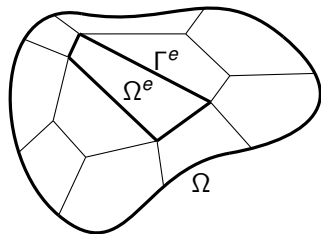
$$\Gamma^{\text{int}} = \bigcup_{e' < e} \bigcup_{e=1}^{n_{el}} \{\Gamma^e \cap \Gamma^{e'}\}$$



# Hybrid Variational Formulation of DEM

- Strong form:

$$(S) : \begin{cases} \text{Find } \mathbf{c} \in H^1(\Omega) \text{ such that} \\ -\kappa \Delta \mathbf{c} + \mathbf{a} \cdot \nabla \mathbf{c} = \mathbf{f}, & \text{in } \Omega \\ \mathbf{c} = \mathbf{g}, & \text{on } \Gamma = \partial\Omega \\ \mathbf{c}_e - \mathbf{c}_{e'} = 0, & \text{on } \Gamma^{\text{int}} \end{cases}$$



- Weak hybrid variational form:

$$(W) : \begin{cases} \text{Find } (\mathbf{c}, \lambda) \in \mathcal{V} \times \mathcal{W} \text{ such that:} \\ a(\mathbf{v}, \mathbf{c}) + b(\lambda, \mathbf{v}) = r(\mathbf{v}) \\ b(\mu, \mathbf{c}) = -r_d(\mu) \\ \text{holds } \forall \mathbf{c} \in \mathcal{V}, \forall \mu \in \mathcal{W}. \end{cases}$$

where

$$a(\mathbf{v}, \mathbf{c}) = (\kappa \nabla \mathbf{v} + \mathbf{v} \mathbf{a}, \nabla \mathbf{c})_{\tilde{\Omega}}$$

$$b(\lambda, \mathbf{v}) = \sum_e \sum_{e' < e} \int_{\Gamma^{e,e'}} \lambda (\mathbf{v}_{e'} - \mathbf{v}_e) d\Gamma + \int_{\Gamma} \lambda \mathbf{v} d\Gamma$$

Notation:

$$\tilde{\Omega} = \bigcup_{e=1}^{n_{el}} \Omega^e$$

$$\tilde{\Gamma} = \bigcup_{e=1}^{n_{el}} \Gamma^e$$

$$\Gamma^{e,e'} = \Gamma^e \cap \Gamma^{e'}$$

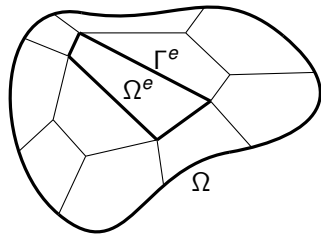
$$\Gamma^{\text{int}} = \bigcup_{e' < e} \bigcup_{e=1}^{n_{el}} \{\Gamma^e \cap \Gamma^{e'}\}$$



# Hybrid Variational Formulation of DEM

- Strong form:

$$(S) : \begin{cases} \text{Find } \mathbf{c} \in H^1(\Omega) \text{ such that} \\ -\kappa \Delta \mathbf{c} + \mathbf{a} \cdot \nabla \mathbf{c} = \mathbf{f}, & \text{in } \Omega \\ \mathbf{c} = \mathbf{g}, & \text{on } \Gamma = \partial\Omega \\ \mathbf{c}_e - \mathbf{c}_{e'} = 0, & \text{on } \Gamma^{\text{int}} \end{cases}$$



- Weak hybrid variational form:

$$(W) : \begin{cases} \text{Find } (\mathbf{c}, \lambda) \in \mathcal{V} \times \mathcal{W} \text{ such that:} \\ a(\mathbf{v}, \mathbf{c}) + b(\lambda, \mathbf{v}) = r(\mathbf{v}) \\ b(\mu, \mathbf{c}) = -r_d(\mu) \\ \text{holds } \forall \mathbf{c} \in \mathcal{V}, \forall \mu \in \mathcal{W}. \end{cases}$$

where

$$a(\mathbf{v}, \mathbf{c}) = (\kappa \nabla \mathbf{v} + \mathbf{v} \mathbf{a}, \nabla \mathbf{c})_{\tilde{\Omega}}$$

$$b(\lambda, \mathbf{v}) = \sum_e \sum_{e' < e} \int_{\Gamma^{e,e'}} \lambda (v_{e'} - v_e) d\Gamma + \int_{\Gamma} \lambda \mathbf{v} d\Gamma$$

Notation:

$$\tilde{\Omega} = \bigcup_{e=1}^{n_{el}} \Omega^e$$

$$\tilde{\Gamma} = \bigcup_{e=1}^{n_{el}} \Gamma^e$$

$$\Gamma^{e,e'} = \Gamma^e \cap \Gamma^{e'}$$

$$\Gamma^{\text{int}} = \bigcup_{e' < e} \bigcup_{e=1}^{n_{el}} \{\Gamma^e \cap \Gamma^{e'}\}$$



# Discretization & Implementation

- Element matrix problem (uncondensed):

$$\begin{pmatrix} \mathbf{k}^{PP} & \mathbf{k}^{PE} & \mathbf{k}^{PC} \\ \mathbf{k}^{EP} & \mathbf{k}^{EE} & \mathbf{k}^{EC} \\ \mathbf{k}^{CP} & \mathbf{k}^{CE} & \mathbf{0} \end{pmatrix} \begin{pmatrix} \mathbf{c}^P \\ \mathbf{c}^E \\ \lambda^h \end{pmatrix} = \begin{pmatrix} \mathbf{r}^P \\ \mathbf{r}^E \\ \mathbf{r}^C \end{pmatrix}$$





# Discretization & Implementation

- Element matrix problem (uncondensed):

$$\begin{pmatrix} \mathbf{k}^{PP} & \mathbf{k}^{PE} & \mathbf{k}^{PC} \\ \mathbf{k}^{EP} & \mathbf{k}^{EE} & \mathbf{k}^{EC} \\ \mathbf{k}^{CP} & \mathbf{k}^{CE} & \mathbf{0} \end{pmatrix} \begin{pmatrix} \mathbf{c}^P \\ \mathbf{c}^E \\ \lambda^h \end{pmatrix} = \begin{pmatrix} \mathbf{r}^P \\ \mathbf{r}^E \\ \mathbf{r}^C \end{pmatrix}$$

Due to the discontinuous nature of  $\mathcal{V}^E$ ,  $\mathbf{c}^E$  can be eliminated at the element level by a static condensation

- Statically-condensed **DEM Element**:

$$\begin{pmatrix} \tilde{\mathbf{k}}^{PP} & \tilde{\mathbf{k}}^{PC} \\ \tilde{\mathbf{k}}^{CP} & \tilde{\mathbf{k}}^{CC} \end{pmatrix} \begin{pmatrix} \mathbf{c}^P \\ \lambda^h \end{pmatrix} = \begin{pmatrix} \tilde{\mathbf{r}}^P \\ \tilde{\mathbf{r}}^C \end{pmatrix}$$



# Discretization & Implementation

- Element matrix problem (uncondensed):

$$\begin{pmatrix} \mathbf{k}^{PP} & \mathbf{k}^{PE} & \mathbf{k}^{PC} \\ \mathbf{k}^{EP} & \mathbf{k}^{EE} & \mathbf{k}^{EC} \\ \mathbf{k}^{CP} & \mathbf{k}^{CE} & \mathbf{0} \end{pmatrix} \begin{pmatrix} \mathbf{c}^P \\ \mathbf{c}^E \\ \lambda^h \end{pmatrix} = \begin{pmatrix} \mathbf{r}^P \\ \mathbf{r}^E \\ \mathbf{r}^C \end{pmatrix}$$

Due to the discontinuous nature of  $\mathcal{V}^E$ ,  $\mathbf{c}^E$  can be eliminated at the element level by a static condensation

- Statically-condensed **DEM Element**:

$$\begin{pmatrix} \tilde{\mathbf{k}}^{PP} & \tilde{\mathbf{k}}^{PC} \\ \tilde{\mathbf{k}}^{CP} & \tilde{\mathbf{k}}^{CC} \end{pmatrix} \begin{pmatrix} \mathbf{c}^P \\ \lambda^h \end{pmatrix} = \begin{pmatrix} \tilde{\mathbf{r}}^P \\ \tilde{\mathbf{r}}^C \end{pmatrix}$$

Computational complexity depends on  $\dim \mathcal{V}^h$  not on  $\dim \mathcal{V}^E$

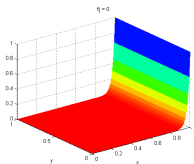


# Angle-Parametrized Enrichment Functions for 2D Advection-Diffusion

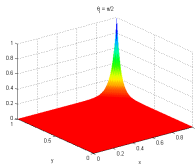
- Derived by solving  $\mathcal{L}c^E = \mathbf{a} \cdot \nabla c^E - \kappa \Delta c^E = 0$  analytically (e.g., separation of variables).

$$c^E(\mathbf{x}; \theta_i) = e^{\left(\frac{a_1 + |\mathbf{a}| \cos \theta_i}{2\kappa}\right)(x - x_{r,i})} e^{\left(\frac{a_2 + |\mathbf{a}| \sin \theta_i}{2\kappa}\right)(y - y_{r,i})} \quad (1)$$

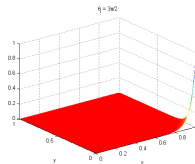
$\Theta^c \equiv \{\theta_i\}_{i=1}^{n^E} \in [0, 2\pi) =$  set of angles specifying  $\mathcal{V}^E$



$$\phi = 0, \theta_i = 0$$



$$\phi = 0, \theta_i = \frac{\pi}{2}$$



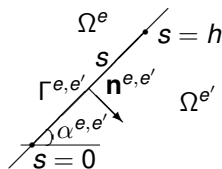
$$\phi = 0, \theta_i = \frac{3\pi}{2}$$

**Figure 2:** Plots of enrichment functions  $c^E(\mathbf{x}; \theta_i)$  for several values of  $\theta_i$  ( $Pe = 20$ )

Parametrization with respect to  $\theta_i$  in (1) enables systematic element design!



# Lagrange Multiplier Approximations



$$\lambda^h \approx \nabla \mathbf{c}_e^E \cdot \mathbf{n}^e = -\nabla \mathbf{c}_{e'}^E \cdot \mathbf{n}^{e'}$$

**Figure 3:** Straight edge  $\Gamma^{e,e'}$   
oriented at angle  $\alpha^{e,e'} \in [0, 2\pi)$

- Trivial to compute given exponential enrichments:

$$\begin{aligned} \lambda^h(s)|_{\Gamma^{e,e'}} &\approx \nabla \mathbf{c}^E \cdot \mathbf{n}|_{\Gamma^{e,e'}} \\ &= \text{const} \cdot \mathbf{e} \left\{ \frac{|\mathbf{a}|}{2\kappa} \left[ \cos(\phi - \alpha^{e,e'}) + \cos(\theta_k - \alpha^{e,e'}) \right] (s - s_r^{e,e'}) \right\} \end{aligned} \quad (2)$$



# Lagrange Multiplier Approximations

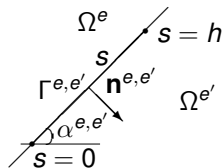


**Figure 3:** Straight edge  $\Gamma^{e,e'}$   
oriented at angle  $\alpha^{e,e'} \in [0, 2\pi)$

$$\lambda^h \approx \nabla c_e^E \cdot \mathbf{n}^e = -\nabla c_{e'}^E \cdot \mathbf{n}^{e'}$$

Limit  $n^\lambda$  to satisfy *inf-sup*:

Use  $\left\lfloor \frac{n^E}{4} \right\rfloor$  Lagrange  
multipliers of the form (2)

- Trivial to compute given exponential enrichments:

$$\begin{aligned} \lambda^h(s)|_{\Gamma^{e,e'}} &\approx \nabla c^E \cdot \mathbf{n}|_{\Gamma^{e,e'}} \\ &= \text{const} \cdot \mathbf{e} \left\{ \frac{|\mathbf{a}|}{2rc} \left[ \cos(\phi - \alpha^{e,e'}) + \cos(\theta_k - \alpha^{e,e'}) \right] (s - s_r^{e,e'}) \right\} \end{aligned} \quad (2)$$

Non-trivial to satisfy *inf-sup* condition:  
the set  $\Theta^c$  that defines  $\mathcal{V}^E$  typically leads to  
too many Lagrange multiplier dofs!



# Mesh Independent Element Design Procedure

## Algorithm 1. "Build Your Own DEM Element"

Fix  $n^E \in \mathbb{N}$  (the desired number of angles defining  $\mathcal{V}^E$ ).

Select a set of  $n^E$  distinct angles  $\{\theta_k\}_{k=1}^{n^E}$  between  $[0, 2\pi)$ .

Set  $\Theta^c = \{\theta_i\}_{i=1}^{n^E}$ .

Define the enrichment functions by:

$$c^E(\mathbf{x}; \Theta^c) = e^{\left(\frac{a_1 + |\mathbf{a}| \cos \Theta^c}{2\kappa}\right)(x - x_{r,i})} e^{\left(\frac{a_2 + |\mathbf{a}| \sin \Theta^c}{2\kappa}\right)(y - y_{r,i})}$$

Determine  $n^\lambda = \left\lfloor \frac{n^E}{4} \right\rfloor$ .

**for** each edge  $\Gamma^{e,e'} \in \Gamma^{\text{int}}$

Compute max and min of  $\frac{|\mathbf{a}|}{2\kappa} [\cos(\phi - \alpha^{e,e'}) + \cos(\theta_k - \alpha^{e,e'})]$ , call them  $\Lambda_{\min}^{e,e'}, \Lambda_{\max}^{e,e'}$ .

Sample  $\{\Lambda_i^{e,e'} : i = 1, \dots, n^\lambda\}$  uniformly in the interval  $[\Lambda_{\min}^{e,e'}, \Lambda_{\max}^{e,e'}]$ .

Define the Lagrange multipliers approximations on  $\Gamma^{e,e'}$  by:

$$\lambda^h|_{\Gamma^{e,e'}} = \text{span} \left\{ e^{\Lambda_i^{e,e'}(s - s_{r,i}^{e,e'})}, 0 \leq s \leq h \right\}$$

**end for**



# Element Nomenclature

## Notation

DGM Element:  $Q\text{-}n^E\text{-}n^\lambda$

DEM Element:  $Q\text{-}n^E\text{-}n^{\lambda+} \equiv [Q\text{-}n^E\text{-}n^\lambda] \cup [Q_1]$

' $Q$ ': Quadrilateral

$n^E$ : Number of Enrichment Functions

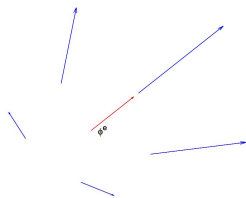
$n^\lambda$ : Number of Lagrange Multipliers per Edge

$Q_1$ : Galerkin Bilinear Quadrilateral Element

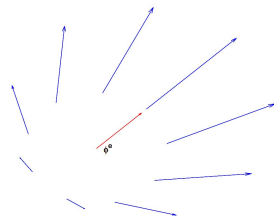
	Name	$n^E$	$\Theta^c$	$n^\lambda$
DGM elements	Q-4-1	4	$\phi + \left\{ \frac{m\pi}{2} : m = 0, \dots, 3 \right\}$	1
	Q-8-2	8	$\phi + \left\{ \frac{m\pi}{4} : m = 0, \dots, 7 \right\}$	2
	Q-12-3	12	$\phi + \left\{ \frac{m\pi}{6} : m = 0, \dots, 11 \right\}$	3
	Q-16-4	16	$\phi + \left\{ \frac{m\pi}{8} : m = 0, \dots, 15 \right\}$	4
DEM elements	Q-5-1 <sup>+</sup>	5	$\phi + \left\{ \frac{2m\pi}{5} : m = 0, \dots, 4 \right\}$	1
	Q-9-2 <sup>+</sup>	9	$\phi + \left\{ \frac{2m\pi}{9} : m = 0, \dots, 8 \right\}$	2
	Q-13-3 <sup>+</sup>	13	$\phi + \left\{ \frac{2m\pi}{13} : m = 0, \dots, 12 \right\}$	3
	Q-17-4 <sup>+</sup>	17	$\phi + \left\{ \frac{2m\pi}{17} : m = 0, \dots, 16 \right\}$	4



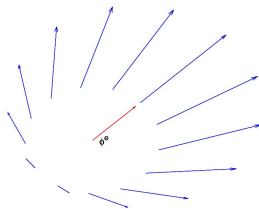
# Illustration of the Sets $\Theta^c$ for the DEM Elements



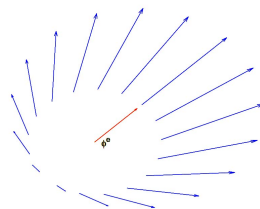
Q-5-1+



Q-9-2+



Q-13-3+



Q-17-4+





# Computational Complexities

Element	Asymptotic # of dofs	Stencil width for uniform $n \times n$ mesh	(# dofs) $\times$ (stencil width)	$L^2$ convergence rate ( <i>a posteriori</i> )
$Q_1$	$n_{el}$	9	$9n_{el}$	2
$Q-4-1$	$2n_{el}$	7	$14n_{el}$	2
$Q_2$	$3n_{el}$	21	$63n_{el}$	3
$Q-8-2$	$4n_{el}$	14	$56n_{el}$	3
$Q-5-1^+$	$3n_{el}$	21	$63n_{el}$	2 – 3
$Q_3$	$5n_{el}$	33	$165n_{el}$	4
$Q-12-3$	$6n_{el}$	21	$126n_{el}$	4
$Q-9-2^+$	$5n_{el}$	33	$165n_{el}$	3 – 4
$Q_4$	$7n_{el}$	45	$315n_{el}$	5
$Q-16-4$	$8n_{el}$	28	$224n_{el}$	5
$Q-13-3^+$	$7n_{el}$	45	$315n_{el}$	4 – 5
$Q-17-4^+$	$9n_{el}$	57	$513n_{el}$	4 – 5

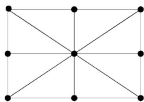


Figure 4:  $Q_1$  stencil

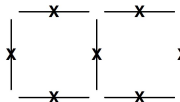


Figure 5:  $Q-4-1$  stencil



# Summary of Computational Properties

## “COMPARABLES”

### *A priori* in computational cost:

- DGM with  $n$  LMs and  $Q_n$
- DEM with  $n$  LMs and  $Q_{n+1}$

### *A posteriori* in convergence rate:

- DGM with  $n$  LMs and  $Q_n$
- DEM with  $n$  LMs and  $Q_n/Q_{n+1}$

- Exponential enrichments  $\Rightarrow$  integrations can be computed analytically.
- $\mathcal{L}c^E = 0 \Rightarrow$  convert volume integrals to boundary integrals:

$$\begin{aligned} a(v^E, c^E) &= \int_{\hat{\Omega}} (\kappa \nabla v^E \cdot \nabla c^E + \mathbf{a} \cdot \nabla c^E v^E) d\Omega \\ &= \int_{\hat{\Gamma}} \nabla c^E \cdot \mathbf{n} v^E d\Gamma \end{aligned}$$



# Homogeneous Boundary Layer Problem

- $\Omega = (0, 1) \times (0, 1)$ ,  $f = 0$ .
- $\mathbf{a} = (\cos \phi, \sin \phi)$ .
- Dirichlet boundary conditions are specified on  $\Gamma$  such that the exact solution to the BVP is given by

$$c_{ex}(\mathbf{x}; \phi, \psi) = \frac{e^{\frac{1}{2\kappa} \{ [\cos \phi + \cos \psi](x-1) + [\sin \phi + \sin \psi](y-1) \}} - 1}{e^{-\frac{1}{2\kappa} [\cos \phi + \cos \psi + \sin \phi + \sin \psi]} - 1}$$

- $\psi \in [0, 2\pi)$  : some flow direction (not necessarily aligned with  $\phi$ ).
- Solution exhibits a sharp exponential boundary layer in the advection direction  $\phi$ , whose gradient is a function of the Péclet number.

Figure 6:  $\phi = \psi = 0$

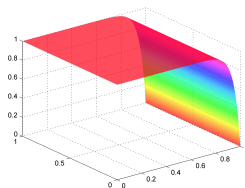
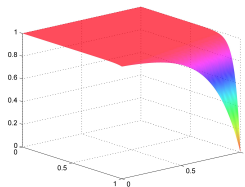
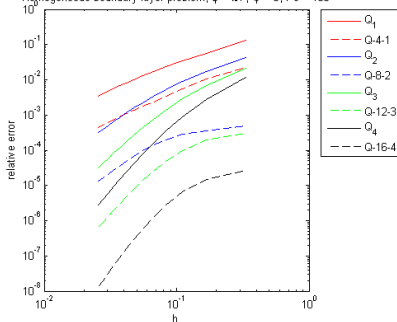


Figure 7:  $\phi = \pi/7, \psi = 0$



# Convergence Analysis & Results ( $\phi = \pi/7, \psi = 0$ )

Homogeneous boundary layer problem,  $\phi = \pi/7, \psi = 0, Pe = 100$



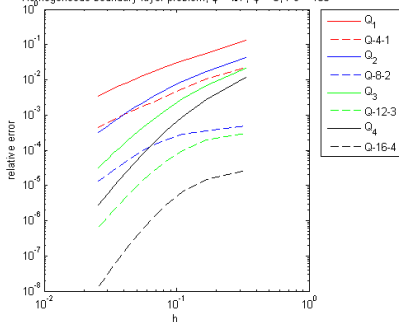
Element	Rate of convergence	# dofs to achieve $10^{-3}$ error
$Q_1$	1.90	63,266
$Q_4-1$	1.99	14,320
$Q_2$	2.38	24,300
$Q_8-2$	3.27	5400
$Q_3$	3.48	12,500
$Q_{12-3}$	3.88	850
$Q_4$	4.41	8600
$Q_{16-4}$	5.19	570

- To achieve for this problem the relative error of 0.1% for  $Pe = 10^3$ :
  - $Q_4-1$  and  $Q_8-2$  require  $\approx 4.5 \times$  **fewer** dofs than  $Q_1$  and  $Q_2$  respectively.
  - $Q_{12-3}$  and  $Q_{16-4}$  require  $\approx 15 \times$  **fewer** dofs than  $Q_3$  and  $Q_4$  respectively.



# Convergence Analysis & Results ( $\phi = \pi/7, \psi = 0$ )

Homogeneous boundary layer problem,  $\phi = \pi/7, \psi = 0, Pe = 100$



Element	Rate of convergence	# dofs to achieve $10^{-3}$ error
$Q_1$	1.90	63,266
$Q_{4-1}$	1.99	14,320
$Q_2$	2.38	24,300
$Q_{8-2}$	3.27	5400
$Q_3$	3.48	12,500
$Q_{12-3}$	3.88	850
$Q_4$	4.41	8600
$Q_{16-4}$	5.19	570

- To achieve for this problem the relative error of 0.1% for  $Pe = 10^3$ :

- $Q_{4-1}$  and  $Q_{8-2}$  require  $\approx 4.5 \times$  **fewer** dofs than  $Q_1$  and  $Q_2$  respectively.

$\Rightarrow 8 \times$  less CPU time.

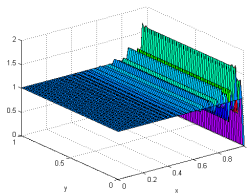
- $Q_{12-3}$  and  $Q_{16-4}$  require  $\approx 15 \times$  **fewer** dofs than  $Q_3$  and  $Q_4$  respectively.

$\Rightarrow 40 \times$  less CPU time.

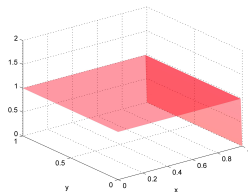


# Solution Plots for Homogeneous BVP

Figure 8:  $\phi = \psi = 0$ ,  $Pe = 10^3$ ,  $\approx 1600$  dofs

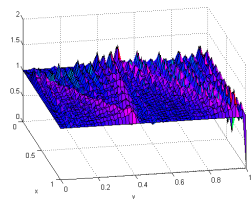


$Q_3$

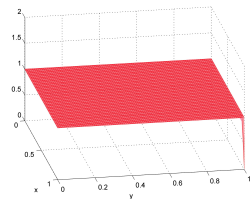


$Q-12-3$

Figure 9:  $\phi = \pi/7$ ,  $\psi = 0$ ,  $Pe = 10^5$ ,  $\approx 1600$  dofs



$Q_3$

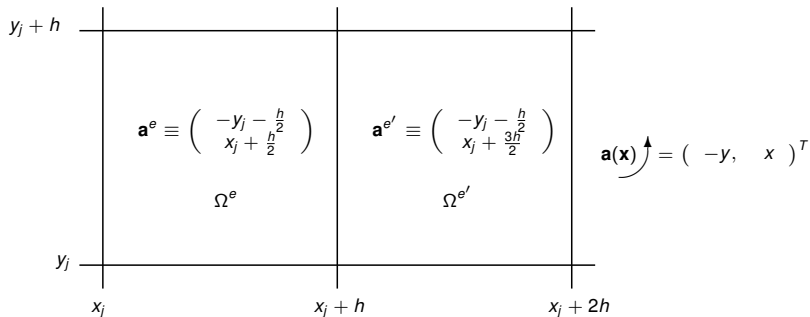


$Q-12-3$



# Extension to Variable-Coefficient Problems

- Define  $\mathcal{V}^E$  *within each element* as the free-space solutions to the homogeneous PDE, with locally-frozen coefficients.
- $\mathbf{a}(\mathbf{x}) \approx \mathbf{a}^e = \text{constant}$  inside each element  $\Omega^e$  as  $h \rightarrow 0$ :  
 $\{\mathbf{a}(\mathbf{x}) \cdot \nabla c - \kappa \Delta c = f(\mathbf{x}) \text{ in } \Omega\} \approx \cup_{e=1}^{n_{el}} \{\mathbf{a}^e \cdot \nabla c - \kappa \Delta c = f(\mathbf{x}) \text{ in } \Omega^e\}.$



- Enrichment in each element:

$$c_e^E(\mathbf{x}; \theta_i^e) = e^{\frac{|\mathbf{a}^e|}{2\kappa} (\cos \phi^e + \cos \theta_i^e)(x - x_{r,i}^e)} e^{\frac{|\mathbf{a}^e|}{2\kappa} (\sin \phi^e + \sin \theta_i^e)(y - y_{r,i}^e)} \in \mathcal{V}_e^E$$



# Inhomogeneous Rotating Advection Problem on an $L$ -Shaped Domain

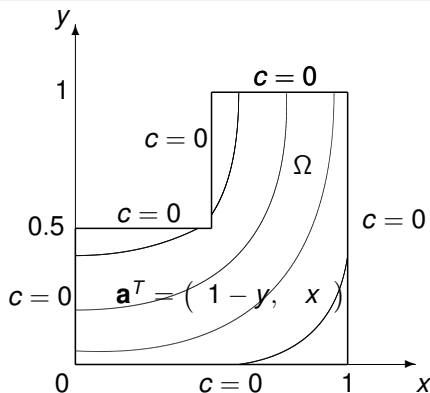


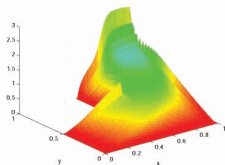
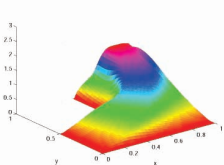
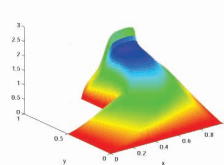
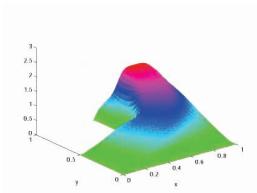
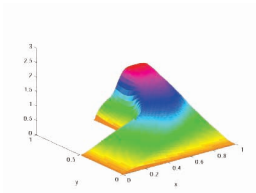
**Figure 10:**  $L$ -shaped domain and rotating velocity field (curved lines indicate streamlines)

- Homogeneous Dirichlet boundary conditions are prescribed on all six sides of  $L$ -shaped domain  $\Omega$ .
- Source:  $f = 1$ .
- $\mathbf{a}^T(\mathbf{x}) = (1 - y, x)$ .
- Outflow boundary layer along the line  $y = 1$ .
- Second boundary layer that terminates in the vicinity of the re-entrant corner  $(x, y) = (0.5, 0.5)$ .





# Solutions Plots for $Pe = 10^3$ with $\approx 3000$ dofs

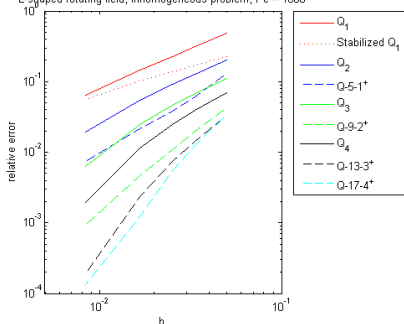
 $Q_1$ Stabilized  $Q_1$  $Q_2$  $Q-5-1^+$  $Q-9-2^+$ 

\* “Stabilized  $Q_1$ ” is upwind stabilized bilinear finite element by Harari *et. al.*



# Convergence Analysis & Results

L-shaped rotating field, inhomogeneous problem,  $Pe = 1000$



Element	Rate of convergence	# dofs to achieve $10^{-2}$ error
$Q_2$	1.94	62,721
$Q-5-1^+$	1.55	21,834
$Q_3$	2.67	33,707
$Q-9-2^+$	2.37	7,568
$Q_4$	3.50	20,796
$Q-13-3^+$	3.23	5,935
$Q-17-4^+$	3.26	4,802

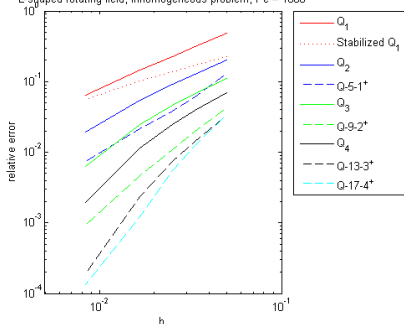
\* "Stabilized  $Q_1$ " is upwind stabilized bilinear finite element proposed by Harari *et. al.*

- To achieve for this problem the relative error of 1% for  $Pe = 10^3$ :
  - $Q-5-1^+$  requires  $2.9 \times$  **fewer** dofs than  $Q_2$  (same **sparsity**).
  - $Q-9-2^+$  requires  $4.5 \times$  **fewer** dofs than  $Q_3$  (same **sparsity**).
  - $Q-13-3^+$  requires  $3.5 \times$  **fewer** dofs than  $Q_4$  (same **sparsity**).



# Convergence Analysis & Results

L-shaped rotating field, inhomogeneous problem,  $Pe = 1000$



Element	Rate of convergence	# dofs to achieve $10^{-2}$ error
$Q_2$	1.94	62,721
$Q_5-1^+$	1.55	21,834
$Q_3$	2.67	33,707
$Q_9-2^+$	2.37	7,568
$Q_4$	3.50	20,796
$Q_{13-3}^+$	3.23	5,935
$Q_{17-4}^+$	3.26	4,802

\* "Stabilized  $Q_1$ " is upwind stabilized bilinear finite element proposed by Harari *et. al.*

- To achieve for this problem the relative error of 1% for  $Pe = 10^3$ :
  - $Q_5-1^+$  requires  $2.9 \times$  **fewer** dofs than  $Q_2$  (same **sparsity**).  
 $\Rightarrow 3.6 \times$  less CPU time.
  - $Q_9-2^+$  requires  $4.5 \times$  **fewer** dofs than  $Q_3$  (same **sparsity**).  
 $\Rightarrow 9.2 \times$  less CPU time.
  - $Q_{13-3}^+$  requires  $3.5 \times$  **fewer** dofs than  $Q_4$  (same **sparsity**).  
 $\Rightarrow 11.4 \times$  less CPU time.



# DEM for the Unsteady Advection-Diffusion Equation

- Unsteady advection-diffusion equation:

$$c_t + \mathbf{a}(\mathbf{x}, t) \cdot \nabla c - \kappa \Delta c = 0$$



# DEM for the Unsteady Advection-Diffusion Equation

- Unsteady advection-diffusion equation::

$$c_t + \mathbf{a}(\mathbf{x}, t) \cdot \nabla c - \kappa \Delta c = 0$$

- Semi-discrete form of PDE (with semi-implicit Euler) at time  $n$ :

$$\frac{c^{n+1} - c^n}{\Delta t} + \mathbf{a}^n(\mathbf{x}) \cdot \nabla c^{n+1} - \kappa \Delta c^{n+1} = 0$$



# DEM for the Unsteady Advection-Diffusion Equation

- Unsteady advection-diffusion equation:

$$c_t + \mathbf{a}(\mathbf{x}, t) \cdot \nabla c - \kappa \Delta c = 0$$

- Semi-discrete form of PDE (with semi-implicit Euler) at time  $n$ :

$$\cancel{\frac{c^{n+1} - c^n}{\Delta t}} + \mathbf{a}^n(\mathbf{x}) \cdot \nabla c^{n+1} - \kappa \Delta c^{n+1} = 0$$

- Enrichment functions inside each element at time step  $n$  are the free-space solutions to steady version of the equation above:

$$\mathcal{V}_e^{E,n} = \text{span}\{c^n(\mathbf{x}) : \mathbf{a}^{n-1}(\bar{\mathbf{x}}_e) \cdot \nabla c^n - \kappa \Delta c^n = 0, \mathbf{x} \in \Omega^e\}$$

where

$\mathcal{V}_e^{E,n}$  = enrichment field inside element  $\Omega^e$  at time step  $n$

$\bar{\mathbf{x}}_e \equiv$  midpoint of element  $\Omega^e$



# Natural Convection in a Differentially-Heated Cavity

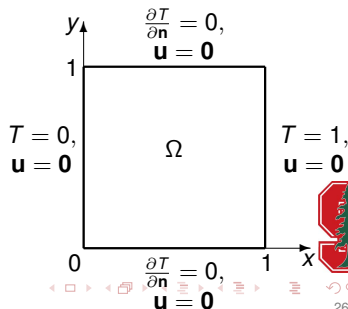
- Incompressible Navier-Stokes equations with Boussinesq temperature approximation.

$$\left\{ \begin{array}{l} \nabla \cdot \mathbf{u} = 0 \\ \frac{\partial \mathbf{u}}{\partial t} + \mathbf{u} \cdot \nabla \mathbf{u} - \frac{1}{Gr^{0.5}} \Delta \mathbf{u} = -\nabla p + T \mathbf{e}_2 \\ \frac{\partial T}{\partial t} + \mathbf{u} \cdot \nabla T - \frac{1}{PrGr^{0.5}} \Delta T = 0 \end{array} \right.$$

where

$\mathbf{u}^T = (u_1(\mathbf{x}, t), u_2(\mathbf{x}, t))$  : fluid velocity vector  
 $p = p(\mathbf{x}, t)$  : fluid pressure  
 $T = T(\mathbf{x}, t)$  : fluid temperature

- $\Omega = (0, 1)^2$ .
- No-slip boundary conditions on  $\mathbf{u}$  on sides of box.
- At time  $t = 0$  begin to heat right wall; top walls of box are insulating (adiabatic).



# Natural Convection in a Differentially-Heated Cavity

- Incompressible Navier-Stokes equations with Boussinesq temperature approximation.

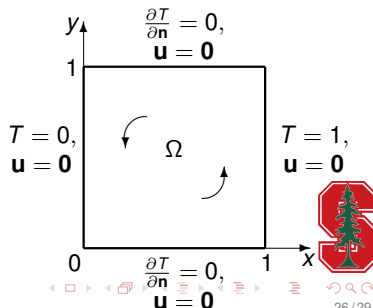
$$\left\{ \begin{array}{l} \nabla \cdot \mathbf{u} = 0 \\ \frac{\partial \mathbf{u}}{\partial t} + \mathbf{u} \cdot \nabla \mathbf{u} - \frac{1}{Gr^{0.5}} \Delta \mathbf{u} = -\nabla p + T \mathbf{e}_2 \\ \frac{\partial T}{\partial t} + \mathbf{u} \cdot \nabla T - \frac{1}{PrGr^{0.5}} \Delta T = 0 \end{array} \right.$$

where

$\mathbf{u}^T = (u_1(\mathbf{x}, t), u_2(\mathbf{x}, t))$  : fluid velocity vector  
 $p = p(\mathbf{x}, t)$  : fluid pressure  
 $T = T(\mathbf{x}, t)$  : fluid temperature

- $\Omega = (0, 1)^2$ .
- No-slip boundary conditions on  $\mathbf{u}$  on sides of box.
- At time  $t = 0$  begin to heat right wall; top walls of box are insulating (adiabatic).

Temperature gradient induces counterclockwise flow field





# Simulation: Galerkin $T$ vs. DGM $T$ ( $Ra = Gr = 1000$ )

$u, v$  : Galerkin  $Q_3$

$p$  : Galerkin  $Q_2$

$T$  : Galerkin  $Q_1$

$T$  : DGM  $Q_4-1$



# Summary

**Discontinuous Enrichment Method (DEM)** =  
efficient, competitive alternative to stabilized FEMs  
for advection-dominated transport problems in CFD.

- Parametrization of exponential basis enables systematic design of DEM elements of arbitrary orders.
- Augmentation of enrichment space with additional free-space solutions can improve further the approximation.
- For all test problems, enriched elements outperform their Galerkin and stabilized Galerkin counterparts of comparable computational complexity, sometimes by many orders of magnitude.
- In a high Péclet regime, DGM and DEM solutions are almost completely oscillation-free, in contrast with the Galerkin solutions.
- Advection-diffusion work generalizable to more complex equations in fluid mechanics (e.g., non-linear, unsteady, 3D).
- Future work: DEM for incompressible Navier-Stokes.



# References

([www.stanford.edu/~irinak/pubs.html](http://www.stanford.edu/~irinak/pubs.html))

- [1] **I. Kalashnikova**, R. Tezaur, C. Farhat. A Discontinuous Enrichment Method for Variable Coefficient Advection-Diffusion at High Peclet Number. *Int. J. Numer. Meth. Engng.* (accepted)
- [2] C. Farhat, **I. Kalashnikova**, R. Tezaur. A Higher-Order Discontinuous Enrichment Method for the Solution of High Peclet Advection-Diffusion Problems on Unstructured Meshes. *Int. J. Numer. Meth. Engng.* **81** (2010) 604-636.
- [3] **I. Kalashnikova**, C. Farhat, R. Tezaur. A Discontinuous Enrichment Method for the Solution of Advection-Diffusion Problems in high Peclet Number Regimes. *Fin. El. Anal. Des.* **45** (2009) 238-250.
- [4] R. Tezaur, C. Farhat. Three-dimensional discontinuous Galerkin elements with plane waves and Lagrange multipliers for the solution of mid-frequency Helmholtz problems. *Int. J. Numer. Methods Engng.* **66** (2006) 796-815.
- [5] C. Farhat, R. Tezaur, J. Toivanen. A domain decomposition method for discontinuous Galerkin discretization of Helmholtz problems with plane waves and Lagrange multipliers. *Int. J. Numer. Method. Engng.* **78** (2009) 1513-1531.
- [6] R. Tezaur, L. Zhang, C. Farhat. A discontinuous method for capturing evanescent waves in multi-scale fluid and fluid/solid problems. *Comput. Methods Appl. Mech. Engng.* **197** (2008) 1680-1698.
- [7] P. Massimi, R. Tezaur, C. Farhat. A discontinuous enrichment method for three-dimensional multiscale harmonic wave propagation problems in multi-fluid and fluid-solid media. *Int. J. Numer. Methods Engng.* **76** (2008) 400-425.
- [8] L. Zhang, R. Tezaur, C. Farhat. The discontinuous enrichment method for elastic wave propagation in the medium-frequency regime. *Int. J. Numer. Methods Engng.* **66** (2006) 2086-2114.

